Experimental and theoretical study of velocity fluctuations during slow movements in humans

Running head: Velocity fluctuations during slow movements

Emmanuel Guigon (https://orcid.org/0000-0002-4506-701X), Oussama Chafik, Nathanaël Jarrassé, Agnès Roby-Brami

Sorbonne Université, CNRS, Institut des Systèmes Intelligents et de Robotique, ISIR, F-75005 Paris, France

Corresponding author:

Emmanuel Guigon

Sorbonne Université, CNRS, Institut des Systèmes Intelligents et de Robotique, ISIR

Pyramide Tour 55 - Boîte Courier 173 - 4 Place Jussieu,75252 Paris Cedex 05, France

Tel: 33 1 44276382 / Fax: 33 1 44275145 / Email: emmanuel.guigon@sorbonne-universite.fr

Conflict of Interest: The authors declare no competing financial interests.

Data availability: Data files are available from Figshare (doi: 10.6084/m9.figshare.5977894).

Abstract

Moving smoothly is generally considered as a higher-order goal of motor control and moving jerkily as a witness of clumsiness or pathology. Yet many common and well-controlled movements (e.g. tracking movements) have irregular velocity profiles with widespread fluctuations. The origin and nature of these fluctuations have been associated with the operation of an intermittent process, but in fact remain poorly understood. Here we studied velocity fluctuations during slow movements using combined experimental and theoretical tools. We recorded arm movement trajectories in a group of healthy participants performing back-and-forth movements at different speeds, and we analyzed velocity profiles in terms of series of segments (portions of velocity between two minima). We found that most of the segments were smooth (i.e. corresponding to a biphasic acceleration), had constant duration irrespective of movement speed and linearly increasing amplitude with movement speed. We accounted for these observations with an optimal feedback control model driven by a staircase goal position signal in the presence of sensory noise. Our study suggests than one and the same control process can explain the production of fast and slow movements, i.e. fast movements emerge from the immediate tracking of a global goal position and slow movements from the successive tracking of intermittently updated intermediate goal positions.

New & Noteworthy

We show in experiments and modeling that slow movements could result from the brain tracking a sequence of via-points regularly distributed in time and space. Accordingly slow movements would differ from fast movement by the nature of the guidance and not by the nature of control. This result could help understanding the origin and nature of slow and segmented movements frequently observed in brain disorders.

Keywords: arm movement, intermittent control, modeling

Introduction

Motor coordination is defined as the ability to control the kinematics and dynamics of multiple degrees of freedom in space and time in order to reach intended goals (Bernstein 1967). Solutions to the coordination problem have been inferred from experimental observations and computational modeling (Todorov and Jordan 2002; Torres and Zipser 2004). A central and popular trend is based on the observed smoothness and gracefulness of goal-directed movements (Flash 1990) which has been turned into the statement that smoothness is a performance index which guides the production of movement (Nelson 1983; Flash and Hogan 1985). Although it is still debated whether movements are planned to be smooth or smoothness is only a by-product of other optimization processes (Uno et al. 1989; Harris and Wolpert 1998), most computational models of motor control produce smooth movements (Harris and Wolpert 1998; Todorov and Jordan 2002; Guigon et al. 2007).

Yet, this "perfect" marriage between experiments and models is probably not the end of the story of motor control. There are at least two reasons for this. First, smoothness is an ill-defined quantity. Many different measures of smoothness exist but not all give a consistent description of actual movement regularity (Balasubramanian et al. 2012). Second, many categories of movement are not smooth, i.e. they are made of segments, units, submovements, and contain multiple velocity peaks, multiple velocity inversions, multiple zero-crossings of acceleration (different terms and quantifications are used in different fields and by different authors): tracking movements (Miall et al. 1985; Doeringer and Hogan 1998), slow movements (Wadman et al. 1979; Morasso et al. 1983; Darling et al. 1988; Vallbo and Wessberg 1993; van der Wel et al. 2009), precision movements (Milner and Ijaz 1990; Boyle et al. 2012a,b), developing and unskilled movements (Clifton et al. 1994; Torres and Andersen 2006), pathological movements (Hallett and Khoshbin 1980; Warabi et al. 1986; Krebs et al. 1999; Shaikh et al. 2015). A common observation is that, for a given amplitude, the velocity profile of the movement changes with duration, i.e. the profile becomes more irregular and contains more peaks as duration increases. This has been observed qualitatively for movements of varying durations obtained by different instructions and conditions: duration imposed by a tempo (Wadman et al. 1979; Darling et al. 1988; van der Wel et al. 2009; Shmuelof et al. 2012; Park et al. 2017; Salmond et al. 2017), duration imposed by velocity instructions (e.g. slow, natural, fast; Darling and Cole 1990; Messier et al. 2003; Ambike and Schmiedeler 2013; Rand and Shimansky 2013), duration constrained by target size (Boyle and Shea 2011; Boyle et al. 2012a,b; Michmizos and Krebs 2014). More quantitatively, several studies have reported an approximate linear relationship between movement duration and different measures of smoothness (number of velocity peaks: van der Wel et al. 2009; Salmond et al. 2017 — number of submovements: Lee et al. 1997; Shmuelof et al. 2012 — frequency of submovement: Meyer et al. 1988 — jerk: Salmond et al. 2017). In these conditions, smoothness increased with average movement velocity (Hernandez et al. 2012; Ambike and Schmiedeler 2013). A consistent result was obtained when movement velocity was directly manipulated in tracking tasks (Miall et al. 1986; Beppu et al. 1987; Vallbo and Wessberg 1993; Asano et al. 2013; see also Doeringer and Hogan 1998; Levy-Tzedek et al. 2010), i.e. slow movements were segmented and segmentation decreased as tracking velocity increased (Miall et al. 1986; see also Doeringer and Hogan 1998; Levy-Tzedek et al. 2010). More specifically, Vallbo and Wessberg (1993) reported a specific temporal organization of slow movements in terms of ~8-10 Hz discontinuities in acceleration profiles which was invariant with respect to movement speed. This proposal is currently the most detailed available description of slow movements.

The main characteristic of movement segmentation is illustrated schematically in Fig. 1A. Both fast and slow movements begin with a rapid increase in velocity and end with a rapid decrease, but they differ by the presence of velocity fluctuations between these two phases which are specific to the slow movements. These fluctuations are not predicted by motor control models that embed an optimization criterion since these models would typically produce movements as shown in Fig. 1B, i.e. smoothness is independent of movement duration. Asymmetric velocity profiles (Harris and Wolpert 1998; Guigon et al. 2007; Berret and Jean 2016) and submovements (Li et al. 2018) are found in some optimal control models, but nothing resembling the results of Fig. 1A has ever been reported. In fact, optimal control does not a priori embed a principle that would make a solution with multiple impulses more optimal than a solution with a single impulse. An attractive concept to account for movement segmentation is the notion of intermittency, i.e. a movement would be composed of a series of "intermittently executed overlapping segments" (Doeringer and Hogan 1998). Yet intermittency has been mainly used as a descriptive principle while computational bases of intermittency remain elusive (see **Discussion**).

The goal of this article is to provide an experimental and computational description of velocity fluctuations during slow movements. Our experimental design resembles that used by Vallbo and Wessberg (1993). While their conclusions were based on a spectral analysis, we perform a fine-scale kinematic analysis of velocity fluctuations. First, we report quantitative experimental observations on movements executed by a group of young, healthy participants. Then we describe a model that gives a detailed account of these observations.

Materials and Methods

Ethics statement

The experiment was approved by the Ethical Assessment Committee at the Sorbonne Université, protocol IRB-20141400001072. Participants signed a consent form prior to participating in the experiment and in accordance with the ethical guidelines of Sorbonne Université and in accordance with the Declaration of Helsinki.

Participants

Ten volunteers (23–28 yr old, 6 male and 4 female) participated in the behavioral experiment. They were all right-hand according to the Edinburgh Protocol of handedness (Oldfield 1971). They had no known neurological disorders and normal or corrected to normal vision and they were uninformed as to the purpose of the experiment.

Apparatus

Participants were seated on a chair and used their right hand to move a stylus on a graphic tablet (54.5 cm diagonal, active area 47.9 × 27.1 cm, resolution 1920 × 1080 pixels; CINTIQ 22HD, Wacom, Vancouver, WA). The flow of the task was controlled by a personal computer running Windows 7 (Microsoft Corporation, USA). The 2D position of the tip of the stylus was recorded at ~130 Hz, resampled by interpolation at 200 Hz to obtain fixed time steps, and stored on the computer for offline processing and analysis using custom written Matlab scripts (Mathworks, Natick, MA, USA).

Experimental procedure

The purpose of the procedure was to induce movements at constant speed. We controlled the speed by manipulations of movement amplitude and duration. As a task with both spatial and temporal constraints can be difficult and elicit odd behaviors (e.g. fast displacements with long pauses to fulfill the temporal constraints, multiple corrections to control spatial precision), we emphasized the temporal over the spatial constraint. At the beginning of a trial, two lines (10 cm long) appeared on the tablet: they were perpendicular to the bottom/left to top/right diagonal and at equal distance from the center of the display. When ready, participants triggered the start of the trial, positioned the tip of the stylus at the center of the bottom/left line, and paced their movements with acoustic cues (frequency 700 Hz, 30 ms, 40 dB) delivered through headphones. The participants were given the instructions of:

1. moving the tip of the stylus periodically between the two lines and perpendicularly to the lines (Fig. 2A), the acoustic cues indicating the time to revert movement direction; 2. moving as smoothly as possible and avoiding terminal corrections to guarantee spatial precision. No instructions were given regarding the contribution of arm segments (shoulder, elbow, wrist) to stylus displacement, yet the movements were dominated by elbow displacements (Salmond et al. 2017). Trial duration was 30 s. Visual feedback of the arm was available and visual feedback of stylus position was drawn online and remained available for the duration of the trial.

Eight task conditions, i.e. eight combinations of movement amplitude (in cm) and *period* (in s), were used: 3.53/2.5, 7.07/3.5, 3.53/1.5, 7.07/2.5, 15/3.5, 7.07/1.5, 15/2.5, 15/1.5 corresponding to mean *speed* (in cm/s): 1.41, 2.02, 2.35, 2.83, 4.29, 4.71, 6, 10. Each condition contained 4 trials (120 s). The conditions were delivered in the indicated order (increasing mean speed). The total acquisition duration was ~40 min, including breaks between trials and between conditions. Prior to data collection, the participants performed several trials to become familiar with the stylus and the task.

Data processing

At this stage, a usual operation is the filtering of the raw data to reveal significant patterns and remove noise and irrelevant patterns. This operation is fundamental as it dictates the timescale of events that will be detected at the data analysis stage (see below). We reviewed a set of studies that analyzed similar types of data. Most of the studies used a low-pass filter with cut-off frequency in the range 5-100 Hz without any justification. In this framework, we proposed a new approach to the choice of the cut-off filtering frequency. This approach, described in the **Results** section, lead to a 9 Hz cut-off frequency. The data were thus filtered with a 4th order Butterworth low-pass filter at 9 Hz.

Velocity, acceleration and jerk were obtained numerically from the two-sample difference of the position, velocity and acceleration signals, respectively.

Data analysis

Filtered kinematic data corresponding to horizontal displacement (displacement along the horizontal dimension of the tablet; Fig. 2A) were processed to quantify movement segmentation. An example of velocity profile (participant NH, movement speed 4.71 cm/s) is shown in Fig. 2B. To simplify processing, we identified unidirectional displacements (positive velocity for a left-to-right displacement, *white box* in Fig. 2B; negative velocity for a right-to-left displacement, *gray box* in Fig. 2B) and we changed the sign of velocity for the right-to-left displacements. We defined a segment as a pulse in the velocity profile, i.e. a portion between two consecutive positive minima (delimited by vertical dashed lines in Fig. 2B and shown schematically in Fig. 2C). Note that segments corresponding to a change in direction were not included in the analysis. A segment was initially described by two elementary quantities: *duration* (time between the two minima), and *velocity* (difference between peak velocity and velocity at start). Note that the terms *duration*/*velocity* are used to describe a segment and the terms *period*/*speed* refer to the overall movement. We added a third quantity (*number of units*, N_{unit}) that characterizes the jerkiness of the pulse, i.e. the number of impulsions that are necessary to produce the pulse. We chose a quantification based on acceleration (rather than jerk) as it is an easily understandable quantity that is lawfully related to force. The number of units is related to the total number of acceleration peaks (in the ascending part of the pulse) and deceleration peaks (in the descending part of the pulse). For instance, a minimum-jerk segment has 2 units. To explain how we calculated N_{unit}, we consider two schematic cases illustrated with velocity, acceleration and jerk profiles (Fig. 2C,D,E and Fig. 2F,G,H). In the case of Fig. 2C, N_{unit} is 4 (Fig. 2D). A more complex case is shown in Fig. 2F. The ascending part has one unit (one acceleration peak) but the acceleration profile is highly irregular (Fig. 2G). In this case, the jerk is decreasing at the start of the segment and a jerk peak occurs before the start of the segment (Fig. 2H, compared to Fig. 2E). We add one unit to account for this irregularity.

Each task condition (i.e. 120 s of back-and-forth movements of given movement speed) can be described by the set of segments it contains and summarized by 3 concise characteristics: 1. the distribution of numbers of units (i.e. how many segments have 2 units, 3 units, ...); 2. the relationship between N_{unit} and duration of the segments; 3. the relationship between N_{unit} and velocity of the segments. The experiment can be described by the influence of movement speed on the distribution of numbers of units, the duration and the velocity of segments.

Statistical analysis

In general, we used classical statistical tests. When necessary, we used Bayesian statistics (ANOVA, linear regression) to assess the evidence for the null hypothesis (absence of effect; see Etz et al. 2018 for a tutorial on Bayesian data analysis). In Bayesian statistics (https://en.wikipedia.org/wiki/Bayes_factor), the ratio B_{10} (Bayes factor) of the likelihood probability of two competing hypotheses H_1 and H_0 (e.g an alternative and a null hypothesis), is calculated to quantify the support for H_1 over H_0. If $B_{10} > 1$, H_1 is more strongly supported by the data under consideration than H_0. In the case when H_0 corresponds an absence of effect, a scale for interpretation of B_{10} is: <0.01 *decisive*=, 0.01-0.03 *very strong*=, 0.03-0.1 *strong*=, 0.1-0.3 *substantial*=, 0.3-1 *anecdotal*=, 1-3 *anecdotal*≠, 3-10 *substantial*≠, 10-30 *strong*≠, 30-100 *very strong*≠, >100 *decisive*≠. If a Bayes factor is for instance < 1, we will say that the evidence is *anecdotal= or better*. Bayes factors were calculated using JASP (JASP 2018).

Results

Compliance with task instructions

The participants performed back-and-forth movements paced by a metronome (Fig. 2B). For each task condition, we calculated the period P and mean speed S (i.e. mean of the velocity signal) of each unidirectional displacement and compared it to the desired period P_d and speed S_d. As P and S were not normally distributed in general (Shapiro-Wilk test), we used a one-sample Wilcoxon rank test. For each participant, we could not reject the null hypothesis that the median of the distribution of $P - P_d$ is 0 ($p < 0.05$) in more than 6/8 conditions (75/80 across participants). Then we performed a regression analysis between P_d and $P - P_d$ across conditions for each participant. The slope (range −0.029/0.023) was non-significantly different from 0 in the 10 participants. Bayes factors (full vs intercept-only regression) were < 1 for the 10 participants. These results indicate that the participants complied with the request of the experimenter.

Movement segmentation

The main results of this experiment are shown in Figs. 3 and 4:

- For a given participant and a given condition (movement speed), the velocity profile was made of segments (Fig. 2B). A large majority of the segments had 2 units (439/558, ~79%), a minority 3 units (98/558, ~18%), and the remainder 4 or more (21/558, ~3%) (Fig. 3A). Mean segment duration increased with N_{unit} (Fig. 3B; correlation coefficient, $r = 0.82$). The distribution of segment duration is shown in Fig. 3C. Segment velocity and N_{unit} were loosely related (Fig. 3D; correlation coefficient, $r = 0.28$). Note that for this participant and this condition, only 3 segments had 5 units (in *blue* in Fig. 3). Accordingly, the mean and std of duration and velocity of 5-unit segments were not meaningful. These observations were robust across participants and conditions. In particular, only a mean of 6/568 segments had 5 units. We did not analyze these results further as they are not directly informative on the strategy used to perform slow movements. Yet it is interesting to note that the model to be described accounts for these results (see Fig. 8).

- For a given participant, the distribution of N_{unit} (Fig. 4A) and the duration of *n*-unit segments ($n = 2$-5; Fig. 4B) varied little with movement speed and the velocity of *n*-unit segments increased with movement speed (Fig. 4C). These observations were robust across participants.

We performed single-participant analysis to assess the statistical strength of these observations:

- We performed a one-factor Bayesian ANOVA on 2-unit segment duration with movement speed as factor. Bayes factors for the 10 participants (Pa) were: Pa_1=0.09 (*strong*=), Pa_2=0.039 (*strong*=), Pa_3=0.004 (*decisive*=), Pa_4=0.016 (*very strong*=), Pa_5=204.4 (*decisive*≠), Pa_6=0.003 (*decisive*=), Pa_7=0.186 (*substantial*=), Pa_8=13.59 (*strong*≠), Pa_9=0.004 (*decisive*=), Pa_{10}=0.000041 (*decisive*=). Analysis of Pa_5 gave a Bayes factor of 0.022 (*very strong*=) when the 1st speed condition is removed. Analysis of Pa_8 gave a Bayes factor of 0.0032 (*decisive*=) when the 3rd speed condition is removed. Post hoc tests gave Bayes factor < 1 (*anecdotal= or better*) in 82% of the comparisons.

- We performed a linear regression between movement speed and 2-unit segment duration. We could not reject the hypothesis that the regression slope is null ($p < 0.05$) in five participants. Bayes factors (full vs intercept-only regression) for the 10 participants were: Pa_1=0.0623 (*strong*=), Pa_2=2.06 (*anecdotal*≠), Pa_3=3.03 (*substantial*≠), Pa_4=0.445 (*anecdotal*=), Pa_5=10227 (*decisive*≠), Pa_6=0.123 (*substantial*=), Pa_7=0.171 (*substantial*=), Pa_8=1.678 (*anecdotal*≠), Pa_9=0.0818 (*strong*=), Pa_{10}=0.04 (*strong*=).

- We performed a linear regression between movement speed and 2-unit segment velocity. Slope range was 0.296/0.439, intercept range -0.22/0.14 and mean R^2 0.187 ($p < 0.001$). We could not reject the hypothesis that the regression intercept is null ($p < 0.05$) in 7/10 participants.

- Similar results were obtained for 3- and 4-unit segments. The 5-unit segments were not included in the statistical analysis due to the small size of the samples.

- Group data were used for comparisons with a model and can be seen in Figs. 7 and 8.

Choice of the cut-off filtering frequency

Our results have been obtained with a specific choice of filtering frequency ($F_s = 9$ Hz, *s* for stylus) and would remain qualitatively similar but quantitatively different for a different filtering frequency (see Salmond 2014; Salmond et al. 2017). We propose the following explanation of our choice (we only describe the method and do not provide experimental results). We can consider the mean duration of the 2-unit segments (which is a well-defined quantity; Fig. 3) as an elementary timescale of motor processing. The most plausible timescale of motor processing should be found when well-identified and easily detectable events (e.g. spikes) trigger elementary motor outputs. For example, simultaneous recordings of single motor unit discharges and correlated fluctuations in force during index finger abduction reveal a specific rise and fall of force after each discharge of a motor unit (Fig. 4 in Galganski et al. 1993). The duration of this elementary pulse of force is around 120 ms. We reproduced the experimental protocol of Galganski (without motor unit recordings). Participants were instructed to exert a constant force (20% MVC) with the index finger on a pinchmeter (P200, Biometrics Ltd, UK; sampling at 1 kHz) guided by a visual feedback. The recorded force profiles (see Fig. 4A in Galganski) were filtered (cut-off frequency F_p, *p* for pinchmeter) and analyzed to identify "force" segments (same method as that used for the velocity profiles recorded with the stylus). The characteristics of segments in the force profiles were qualitatively similar to those found in the velocity profiles. We adjusted F_p so that the mean duration of 2-unit "force" segments is 120 ms. We found $F_p = 10$ Hz. F_p can be considered as an appropriate filtering frequency for force signals recorded at 1 kHz. Then we reproduced our velocity experiment using an accelerometer (ACL300, Biometrics Ltd, UK; sampling at 1 kHz) as measurement system. The recorded acceleration profiles were integrated to obtain velocity profiles which were filtered (cut-off frequency $F_a = F_p = 10$ Hz, a for accelerometer) and analyzed to identify "velocity" segments. Again the characteristics of segments recorded with the accelerometer were qualitatively similar to those found in the velocity profiles recorded with the stylus. On this basis we adjusted F_s so that the mean duration of 2-unit segments in the stylus experiment is equal to the mean duration of 2-unit segments in the accelerometer experiment. We found $F_s = 9$ Hz. This value of cut-off frequency was actually used for data processing (see **Data processing**).

To confirm this method, we calculated the power spectral density function of the unfiltered acceleration signal. For one participant, there was a broad spectrum between 4 and 12 Hz with a peak around 8 Hz for all task conditions (Fig. 5A). Across participants, peak frequency varied little with movement speed, with a mean of 8.05 Hz (Fig. 5B). This observation indicates the putative presence of events of ~120 ms duration in the acceleration signal, and lends some independent support to the methodology described above and to our choice of cut-off frequency.

Modeling

In order to make sense of these results, we developed a computational model based on optimal feedback control theory (see **Discussion** for alternative models). We used the framework of control theory (Todorov 2004), i.e. we considered an object to be controlled with dynamics

$$\frac{d\boldsymbol{x}(t)}{dt} = \boldsymbol{f}(\boldsymbol{x}(t), \boldsymbol{u}(t)) + \boldsymbol{n}_{dyn}(t),$$

where $\boldsymbol{x}$ is the state of the object, $\boldsymbol{f}$ a function, $\boldsymbol{n}_{dyn}$ a noise term, and $\boldsymbol{u}$ an input defined by the control policy

$$\boldsymbol{u}(t) = \boldsymbol{\pi}(\boldsymbol{x}^*(t), \hat{\boldsymbol{x}}(t)),$$

where $\boldsymbol{x}^*$ is the goal state and $\hat{\boldsymbol{x}}$ the estimated state of the object (*italic* is used for scalars, ***bold italic*** for vectors, and **bold** for matrices). If $\boldsymbol{f}$ describes the dynamics of a moving limb and $\boldsymbol{\pi}$ tracks a goal (e.g. trajectory, fixed point), the model produces displacements which can be analyzed in terms of segments and compared to the experimental data. We chose for $\boldsymbol{\pi}$ an optimal feedback control policy (combined with an optimal state estimator), i.e. at each time t between t_0 and t_f, the input $\boldsymbol{u}$ minimizes the cost function

$$J(\boldsymbol{u}) = \int_t^{t_f} L\big(\boldsymbol{x}(\xi), \boldsymbol{u}(\xi)\big) d\xi,$$

subject to object dynamics, with boundary conditions $\boldsymbol{x}(t_0) = \boldsymbol{x}_0$, $\boldsymbol{x}(t) = \hat{\boldsymbol{x}}(t)$ and $\boldsymbol{x}(t_f) = \boldsymbol{x}^*(t)$, where L is a positive function. The rationale for this choice is to consider a controller that solves central problems of motor control (trajectory formation, degree-of-freedom problem, structured variability; Hoff and Arbib 1993; Todorov and Jordan 2002; Liu and Todorov 2007; Guigon et al. 2008a,b; Izawa et al. 2008). The quantity $t_f - t$ defines the prediction horizon of control. If t_f is fixed, the prediction horizon decreases as the controlled object approaches its goal. In this case, the control policy is nonstationarity and lacks the required flexibility in time observed in motor control (Torres and Andersen 2006; Guigon 2010; Rigoux and Guigon 2012). This issue can be addressed using an infinite-horizon formulation of optimal control (i.e. $t_f = +\infty$; Rigoux and Guigon 2012; Qian et al. 2013). Here we exploited the notion of receding horizon (i.e $t_f = t + T_{\mathrm{H}}$, where T_{H} is a fixed duration) which corresponds to a fixed prediction horizon ($t_f - t = T_{\mathrm{H}}$). This means that at each time, there is a fixed duration T_{H} to reach the intended goal, irrespective of the time already spent for this goal. Control with a receding horizon defines model predictive control

(Camacho and Bordons 1999), and has already been used in models of motor control (Bye and Neilson 2008, 2010; Berio et al. 2017).

As it is formulated, the model has a single free parameter T_H, and, in the case of a second-order linear dynamics ($\boldsymbol{f}$) and quadratic cost (L), would produce smooth velocity profiles as T_H is varied (e.g. Fig. 1B). In detail, the state $\boldsymbol{x}$ is a vector of position and velocity $[p\ v]^T$, $\boldsymbol{x}_0 = [p_0\ 0]^T$, and $\boldsymbol{x}^* = \left[p_f\ 0\right]^T$, where p_0 and p_f define the initial and final positions, respectively. There is evidence that only the fastest movements are smooth (see **Introduction**), which suggests that T_H is constant.

The model can be used without modifications to produce a movement of a given amplitude (or duration) at constant speed. The principle is to set the goal velocity to the intended movement speed and increment periodically the goal position by a fixed quantity equal to the expected displacement in a period at the given speed. Formally, we note s the movement speed and T_I the period. In the case of a second-order dynamics, the goal state $\boldsymbol{x}^*(t)$ is the vector $[p^*(t)\ v^*(t)]^T$. We set $v^*(t) = s$ and

$$p^*(t) = sT_\mathrm{I} \sum_{k=0}^{N} h(t - kT_\mathrm{I}),$$

where h is the step function ($h(t) = 0$ if $t < 0$ otherwise $h(t) = 1$) and $N = \lfloor D/T_\mathrm{I} \rfloor$ (for given movement duration D) or $N = \lfloor A/s/T_\mathrm{I} \rfloor$ (for given movement amplitude A). In fact, the goal position is a regular staircase signal. Note that the control principle is not to follow instantaneously the trajectory defined by the goal state, but to reach the goal state defined at each time t at the horizon $t + T_\mathrm{H}$. The staircase signal can be considered as a sequence of via-points regularly distributed in time and space.

We simulated the model for an inertial point actuated by a linear muscle, i.e.

$$\boldsymbol{f}\big(\boldsymbol{x}(t),u(t)\big)=\begin{cases}\dot{x}_1=x_2\\ m\dot{x}_2=x_3\\ \tau\dot{x}_3=-x_3+x_4\\ \tau\dot{x}_4=-x_4+u\end{cases}$$

where m and τ are parameters, with $L(\boldsymbol{x},u)=u^2$. State estimation was defined by

$$\dot{\hat{\boldsymbol{x}}}(t)=\boldsymbol{f}\big(\hat{\boldsymbol{x}}(t),u(t)\big)+\mathbf{K}\big(\boldsymbol{y}(t)-\mathbf{H}\hat{\boldsymbol{x}}(t)\big),$$

where $\mathbf{K}$ is the Kalman gain, $\mathbf{H}$ the observation matrix, and

$$\boldsymbol{y}(t)=\mathbf{H}\boldsymbol{x}(t)+\boldsymbol{n}_{obs}(t),$$

where $\boldsymbol{n}_{obs}$ is a noise term. Parameters were $m=1$ kg, $\tau=0.05$ s, $T_{\mathrm{H}}=0.28$ s, and $T_{\mathrm{I}}=0.13$ s, and $\mathbf{H}$ is the 4×4 identity matrix.

We first considered the noise-free case. Simulated position and velocity profiles for 4 movement speeds (1, 2, 5, 10 cm/s) are shown in Fig. 6A,B. The staircase goal position $p^*(t)$ and the constant goal velocity $v^*(t)$ are shown only for the fastest movement in Fig. 6A,B. The velocity profiles were segmented. All the segments had 2 units. Their duration was constant (~130 ms) independent of movement speed (Fig. 6C) and their velocity increased linearly with movement speed (Fig. 6D). Segment duration was strictly determined by T_{I}. The slope of the speed/velocity relationship decreased with T_{H}.

The deterministic model provides an elementary mechanism that can partially account for the experimental observations. In fact, the model cannot explain the existence of segments with more than 2 units and properties related to variability (Fig. 3). An hypothesis is that the existence of segments with more than 2 units and the observed variability in segment duration, velocity and N_{unit} are due to the corruption of a nominal deterministic process by noise. We explored this issue using a classic approach to noise modeling, i.e. dynamic (motor) and observation (sensory) noises contained an additive (signal-independent) term and a multiplicative (signal-dependent) term, and had Gaussian distributions (Todorov 2005; Guigon et al. 2008a,b). Multiplicative sensory noise is an instantiation of Weber's law

(Burbeck and Yap 1990). Many parameters are necessary to specify noise properties. A thorough exploration of these parameters is a daunting task and would not lead to a decisive conclusion due to the highly simplified nature of the model. We proceeded in the following way. We tested each type of noise separately. We observed that: 1. Gaussian noise has too fast variations and needs to be filtered (time constant 0.05 s); 2. additive observation noise does not create segments with more than 2 units; 3. additive dynamic noise creates segments with more than 2 units but all the segments have the same duration irrespective of N_{unit}; 4. multiplicative dynamic noise has a deleterious effect on control. This latter observation does not contradict the fact that signal-dependent noise plays a central role in motor control (Harris and Wolpert 1998; Todorov and Jordan 2002). In fact, slow movements (as compared to fast movements) are produced by weak signals, and a large and probably unrealistic quantity of signal-dependent noise is necessary to induce variability for these movements.

We ran simulations with multiplicative observation noise (same conditions and parameters as in noise-free simulations; $D = 240\,s$). We considered the noise model described in Guigon et al. (2008a). Multiplicative observation noise is given by

$$\boldsymbol{n}_{obs}(t) = \sum_{i=1}^{2} \zeta_i(t)\mathbf{D}_{\boldsymbol{i}}\boldsymbol{x}(t),$$

where $\boldsymbol{\zeta} = [\zeta_1\ \zeta_2]$ is a zero-mean Gaussian random vector with covariance matrix Ω^{ζ}, and $\mathbf{D}_{\boldsymbol{i}}$ a 4x4 matrix. We took

$$\Omega^{\zeta} = \sigma_{noise}\begin{bmatrix} 1 & 0 \\ 0 & 1 \end{bmatrix}$$

and

$$\mathbf{D}_1 = \begin{bmatrix} 1 & 0 & 0 & 0 \\ 0 & 0 & 0 & 0 \\ 0 & 0 & 0 & 0 \\ 0 & 0 & 0 & 0 \end{bmatrix} \text{ and } \mathbf{D}_2 = \begin{bmatrix} 0 & 0 & 0 & 0 \\ 0 & 10 & 0 & 0 \\ 0 & 0 & 0 & 0 \\ 0 & 0 & 0 & 0 \end{bmatrix}.$$

For comparison, we built an average participant. We found a set of noise parameters that satisfactorily accounts for the average experimental observations ($\sigma_{noise} = 0.45$; Figs. 7,8). Figures 7 and 8 show that the model qualitatively captures the properties of segments: distribution of number of units (Fig. 7A), invariance of segment duration with movement speed (Fig. 7B), scaling of segment velocity with movement speed (Fig. 7C,D,E,F), relationship between N_{unit} and duration (Fig. 8A), relationship between N_{unit} and velocity (Fig. 8B). There are several reasons why some of the trends in the experimental data are not captured by the model. First, we did not attempt to find the best fit which would not be especially meaningful due to the highly simplified nature of the model (linear dynamics, Gaussian noise, ...). Second we observed that the power spectrum of simulated acceleration was almost exclusively concentrated at a single frequency around 8 Hz, which suggests that other forms of variability should be considered. Third, the range of movement speed (1-10 cm/s) might not be entirely homogeneous at all levels of data analysis. Fourth, we have built a "mean" participant for comparison with the model. Due to the averaging process, characteristics of the mean participant may differ from those of any single participant.

We note that the model is linear and thus invariant relative to movement speed. Accordingly, it does not predict a change in behavior (segmentation) as movement speed increases. This may not be a limitation of the model (see **Discussion**).

Discussion

In summary, our results show that: 1. movements in a certain range of speeds are made of segments defined as pulses in the velocity profile; 2. the segments are made of units defined from peaks in the acceleration and jerk profiles, and most of the segments have only two units (i.e. one acceleration and one deceleration phase); 3. the duration of the segments depends on their number of units and not on instructed movement speed; 4. the velocity of the segments scales with movement speed. A model explains these results by the optimal tracking of a staircase goal position signal in the presence of sensory noise.

Task design

The starting point of this study is the observation that there exists a large class of nonsmooth movements whose properties are not well explained by current computational approaches. Yet this class is not homogeneous as it encompasses movements of various velocities and governed by various instructions. The only common property is that of being markedly slower than the fastest possible movements (see **Introduction**). Here, we studied linear movements in a specific range of mean velocity (1.4-10 cm/s). This range overlaps with ranges used in previous studies of so-called "slow" movements (Vallbo and Wessberg 1993; Doeringer and Hogan 1998; Park et al. 2017) and corresponds to movements with pervading velocity fluctuations (Fig. 2B). As in Park et al. (2017), our participants were instructed to match the period of a metronome. In other studies, the participants tracked a "velocity" reference (Vallbo and Wessberg 1993; Doeringer and Hogan 1998). In preliminary experiments, we tested participants in a tracking task and found little difference with the metronome task.

What are "slow movements"?

We have repeatedly used the term "slow movements" as a proxy for a large and inhomogeneous class of movements, but we lack a definition of these movements. The proposed model suggests as a definition that a slow movement is a movement guided by partial successive goal position and velocity signals (the staircase position and the constant velocity signals), irrespective of the global goal defined by the desired duration and amplitude of the movement. By contrast, a fast movement is guided by a single stair corresponding to the global goal of the movement. An analogy with stair climbing is instructive. A slow movement would correspond to stair-by-stair climbing until the next floor, a fast movement to a direct jump to the next floor.

According to the model, the only condition for segmentation is the presence of a staircase goal position signal. Since the model is linear, the actual size of a stair (and thus movement speed) has no direct influence on segmentation. Although it can be considered as a limitation of the model, an alternative view is that the very mechanism of the model (the control policy) is not sensitive to movement speed, but the choice of the goal position and velocity signals (stair-by-stair vs direct jump) is. In fact, this property can be considered as a prediction of the model. The characteristics of segmentation (distribution of number of units, Fig. 4A; invariance of segment duration, Fig. 4B; scaling of segment velocity, Fig. 4C) should not change as movement speed increases as long as the movement is performed as a slow movement. In this framework, a slow movement would be defined as a movement of sufficient duration so that the participant focuses locally on the control of velocity (as defined by the presence of characteristic fluctuations in the velocity profile) rather than globally on the spatial goal of the movement. In our experimental protocol, we observed velocity fluctuations for durations > 1.5 s, which, given the size of the tablet, corresponds to movement speeds < 10 cm/s. Using free arm movements rather than movements on a tablet, we could obtain a much larger range of amplitude and thus a larger range of speed.

An open question is whether the reported characteristics of slow movements might be specific to our experimental procedure and related to an unusual, artificial mean of producing movement. We believe this is not the case for two reasons. First, the procedure induces a similar behavior and similar movement properties in all participants. Furthermore, in preliminary experiments, we observed that movements obtained in tracking a slowly moving target had similar properties than movements in the metronome task. Second, our results are consistent with those of previous studies in which slow movements were induced by various means (tempo, instructions, target size; see **Introduction**).

Here we considered a comparison between slow and fast *discrete* movements (i.e movements that terminate with zero speed and acceleration), and did not address the distinction between *discrete* and *rhythmic* movements (Guiard 1993; Hogan and Sternad 2007). In fact, as the speed of the movement increases with the frequency of the metronome, our slow movements should transform into rhythmic rather than discrete movements. Yet neither our results nor our model provide new insights into this distinction.

Time invariance

We observed that changes in instructed movement speed did not modify the temporal structure of movement segmentation, i.e. segment duration remained unchanged as speed increased while segment velocity scaled with speed. The strategy to increase movement speed is thus to produce segment of constant duration and longer amplitude. This strategy confirms the results of Vallbo and Wessberg (1993) who observed velocity and acceleration profiles with discontinuities at 8-10 Hz independent of movement speed. Their conclusions based on frequency analysis are supported here by both frequency and fine-scale kinematic analysis. This strategy is also consistent with the notion of isochrony, i.e. changes in velocity scale with amplitude in order to keep movement duration constant, which is an ordinary feature of different types of movement (Binet and Courtier 1893; Stetson and McDill 1923; Denier van der Gon and Thuring 1965; Glencross 1975; Freund and Büdingen 1978; Viviani and Terzuolo 1982; Jeannerod 1984; Gordon and Ghez 1987; Sartori et al. 2013). The origin of isochrony is unknown. In the model, isochrony results from a rhythmic goal position signal. Interestingly the clearest examples of isochrony are found in motor activities with prevalent underlying rhythms, e.g. eyelid movements (Gruart et al. 2000), handwriting (Freeman 1914), typing (Terzuolo and Viviani 1980), speech (Alexandrou et al. 2016).

The results of Krebs et al. (1999) are highly relevant to the present study. They analyzed slow movements of individuals with brain damaged and concluded that sub-movements speed profile was invariant and that the sub-movements shapes were unaffected by peak speed. Yet the duration of submovements was not reported. We analyzed original data from Krebs (1997). Krebs (1997) reported total movement amplitude, total movement duration, submovement peak velocity and submovement duration for different participants (control, stroke patients). From these data, we calculated mean movement speed (total amplitude/total duration). There is a clear scaling of submovement peak velocity with movement speed, but there is no clear invariance of submovement duration. A central difference with our results is the range of submovement duration (0.5-1 s in Krebs vs 0.1-0.5 s here).

Intermittency, discontinuity, pulsatile control

Our results and our model are consistent with notions such as intermittency, discontinuity and pulsatile control which have been proposed to account for the apparently discrete nature of motor control (Navas and Stark 1968; Neilson et al. 1988; Vallbo and Wessberg 1993; Welsh and Llinás 1997; Doeringer and Hogan 1998; Cabrera and Milton 2002; Gross et al. 2002; Loram and Lakie 2002; Jaberzadeh et al. 2003; Fishbach et al. 2007; Bye and Neilson 2010; Karniel 2013). Yet most studies used these notions in a purely descriptive way. Some computational accounts of intermittency have been proposed for the control of unstable dynamics (quiet standing, stick balancing, virtual unstable objects, ...; Cabrera and Milton 2002; Bottaro et al. 2008; Asai et al. 2009; Gawthrop et al. 2011), and trajectory tracking (Bye and Neilson 2010; Sakaguchi et al. 2015). The central idea in these proposals is the existence of "open-loop" periods, i.e. periods during which no control is applied (act-and-wait; Asai et al. 2009) or feedback is not processed (Gawthrop et al. 2011), which can be triggered or stopped by a clock or by a specific event (e.g. threshold crossing). Here we propose a different view of intermittency. Intermittent control is defined as the guidance of a continuous closed-loop controller by a rhythmic goal signal. Closed-loop control is deemed necessary for the model to solve central problems of motor control (Todorov and Jordan 2002). Accordingly one and the same controller can produce fast and slow movements. The central element of intermittency is the ~8 Hz rhythmic goal signal and could correspond to oculomotor signals indicating anticipatory eye movements or signals contributing to eye-hand coordination (McCauley et al. 1999a,b). The neurophysiological origin of this signal is unknown. Vallbo and Wessberg (1993) thoroughly addressed the 8-10 Hz discontinuities in the kinematics of slow movements and physiological tremor, and concluded that they have not the same nature. They argued that the observed discontinuities are of supraspinal origin, and result from the action of a biphasic pulse generator functioning at regular rate. Primary motor cortex is a likely source of inputs to the spinal cord in this range of frequency (Conway et al. 1995). Furthermore, there is a significant coherence between finger acceleration and activity in local field potentials and single units in monkey motor cortex during slow finger movements (Williams et al. 2009). Yet multiple brain regions (e.g. in the cerebellum and the reticular formation) may contribute to the production of discontinuities (Williams et al. 2010).

Alternative explanations

An open question is whether there are alternative ways to explain our experimental results. Irrespective of the theoretical framework (except pure open-loop control), a movement of a system is a consequence of a discrepancy between the current state of the system and a goal state. In the task dynamics framework (Kelso 1995), the discrepancy is defined by the distance to an attractor state of the system (fixed point, limit cycle) and the spatiotemporal characteristics of the movement are an emergent property of the dynamics of the attractor. A dynamical system with a limit cycle attractor can produce slow rhythmic movements, but it will not by itself generate velocity fluctuations. In the control theory framework, the discrepancy is the distance between the current state and the goal state. The movement can be produced either by a fixed gain (e.g. Proportional-Derivative controller) or by a time-varying gain (e.g. optimal feedback controller). Consider first the case where the goal state is fixed. The PD controller generates an oscillatory pattern whose frequency is determined by the gain. Appropriate damping can transform this pattern into a slow displacement toward the goal. The optimal feedback controller generates a smooth displacement whose velocity is dictated by the chosen time horizon (Fig. 1B). There are no mechanisms in these controllers to produce velocity fluctuations. If the goal is a staircase signal, both controllers produce slow displacements with velocity fluctuations, although the fluctuations correspond to abrupt (nonsmooth) changes in velocity in the case of the PD controller.

An alternative view would be that fluctuations result from intermittent motor commands or intermittent updates in the feedback loop (see above; Asai et al. 2009; Gawthrop et al. 2011). In these scenarii, the fluctuations are produced by periods of open-loop control during which the dynamics of the system (e.g. an inverted pendulum) is not or only approximately controlled. These approaches are pertinent for the control of unstable dynamics but have no direct counterpart for the control of stable dynamics. It is still unclear whether different types of intermittency are necessary in motor control, e.g. intermittent open-loop control to exploit the dynamics of unstable objects vs intermittent closed-loop control for stable objects.

Rationale for the staircase goal signal

The model is based on the idea that motor control results from the interplay between a "universal", task-independent controller (e.g. optimal feedback controller) and a task representation in terms of goals (Todorov and Jordan 2002). In this framework, we have translated the task at hand (movements of constant velocity) into a set of via-points that indicate partial successive goals. In fact, to produce a movement at constant speed, the controller needs to track goals on a constant-speed trajectory, i.e. a staircase positional signal and constant velocity signal. The staircase signal needs not be regular although this is the simplest solution. In this case, the only open parameter is the frequency of the staircase signal.

The staircase signal is considered as a computational necessity. But is it a physiological necessity? If we consider the problem from the point of view of the nervous system, it is clear that there are some constraints on the motor control machinery that prevent the production of smooth movements of arbitrary duration. The origin of such a limitation is unknown but we can speculate that it is related to the rhythmic and pulsatile nature of neural processes (Vallbo and Wessberg 1993; Gross et al. 2002) which plays a prevalent role in the production of skilled actions (Shaffer 1982), e.g. handwriting (Freeman 1914), typing (Terzuolo and Viviani 1980), speech (Alexandrou et al. 2016). In this framework, the staircase signal can be considered as a task representation adapted to the properties of the sensorimotor apparatus.

References

Alexandrou AM, Saarinen T, Kujala J, Salmelin R. A multimodal spectral approach to characterize rhythm in natural speech. *J Acoust Soc Am* 139: 215-226, 2016. doi: https://dx.doi.org/10.1121/1.4939496

Ambike S, Schmiedeler JP. Invariant geometric characteristics of spatial arm motion. *Exp Brain Res* 229: 113-124, 2013. doi: https://dx.doi.org/10.1007/s00221-013-3599-9

Asai Y, Tasaka Y, Nomura K, Nomura T, Casadio M, Morasso P. A model of postural control in quiet standing: Robust compensation of delay-induced instability using intermittent activation of feedback control. *PLoS One* 4: e6169, 2009. doi: https://dx.doi.org/10.1371/journal.pone.0006169

Asano T, Izawa J, Sakaguchi Y. Mechanisms for generating intermittency during manual tracking task. In: *Advances in Cognitive Neurodynamics III*, edited by Yamaguchi Y. Dordrecht: Springer, 2013, p. 559-566. doi: https://dx.doi.org/10.1007/978-94-007-4792-0_75

Balasubramanian S, Melendez-Calderon A, Burdet E. A robust and sensitive metric for quantifying movement smoothness. *IEEE Trans Biomed Eng* 59: 2126-2136, 2012. doi: https://dx.doi.org/10.1109/TBME.2011.2179545

Beppu H, Nagaoka M, Tanaka R. Analysis of cerebellar motor disorders by visually-guided tracking movement. II. Contribution of the visual cues on slow ramp pursuit. *Brain* 110: 1-18, 1987. doi: https://dx.doi.org/10.1093/brain/110.1.1

Berio D, Calinon S, Fol Leymarie F. Generating calligraphic trajectories with model predictive control. In: *Proc 43rd Conference on Graphics Interface*, pp 132-139, 2017. doi: https://dx.doi.org/10.20380/GI2017.17

Bernstein N. *The Co-ordination and Regulation of Movements*. Oxford, UK: Pergamon Press, 1967.

Berret B, Jean F. Why don't we move slower? The value of time in the neural control of action. *J Neurosci* 36: 1056-1070, 2016. doi: https://dx.doi.org/10.1523/JNEUROSCI.1921-15.2016

Binet A, Courtier J. Sur la vitesse des mouvements graphiques. *Revue Philosophique* 35: 664-671, 1893. link: http://www.jstor.org/stable/41075629

Bottaro A, Yasutake Y, Nomura T, Casadio M, Morasso P. Bounded stability of the quiet standing posture: An intermittent control model. *Hum Mov Sci* 27: 473-495, 2008. doi: https://dx.doi.org/10.1016/j.humov.2007.11.005

Boyle J, Kennedy D, Shea CH. Optimizing the control of high ID movements: Rethinking the obvious. *Exp Brain Res* 223: 377-387, 2012a.

doi: https://dx.doi.org/10.1007/s00221-013-3712-0

Boyle J, Panzer S, Wright D, Shea CH. Extended practice of reciprocal wrist and arm movements of varying difficulties. *Acta Psychol (Amst)* 140: 142-153, 2012b.
doi: https://dx.doi.org/10.1016/j.actpsy.2012.03.006

Boyle JB, Shea CH. Wrist and arm movements of varying difficulties. *Acta Psychol (Amst)* 137: 382-396, 2011.
doi: https://dx.doi.org/10.1016/j.actpsy.2011.04.008

Burbeck C, Yap Y. Two mechanisms for localization? Evidence for separation-dependent and separation-independent processing of position information. *Vis Res* 30: 739-750, 1990.
doi: https://dx.doi.org/10.1016/0042-6989(90)90099-7

Bye RT, Neilson PD. The BUMP model of response planning: Variable horizon predictive control accounts for the speed-accuracy tradeoffs and velocity profiles of aimed movement. *Hum Mov Sci* 27: 771-798, 2008.
doi: https://dx.doi.org/10.1016/j.humov.2008.04.003

Bye RT, Neilson PD. The BUMP model of response planning: Intermittent predictive control accounts for 10 Hz physiological tremor. *Hum Mov Sci* 29: 713-736, 2010.
doi: https://dx.doi.org/10.1016/j.humov.2010.01.006

Cabrera JL, Milton JG. On-off intermittency in a human balancing task. *Phys Rev Lett* 89: 158702, 2002.
doi: https://dx.doi.org/10.1103/PhysRevLett.89.158702

Camacho EF, Bordons C. *Model Predictive Control*. London, UK: Springer, 1999.
isbn: http://www.isbnsearch.org/isbn/9783540762416

Clifton RK, Rochat P, Robin DJ, Berthier NE. Multimodal perception in the control of infant reaching. *J Exp Psychol: Hum Percept Perform* 20: 876-886, 1994.
doi: https://dx.doi.org/10.1037//0096-1523.20.4.876

Conway BA, Halliday DM, Farmer SF, Shahani U, Maas P, Weir AI, Rosenberg JR. Synchronization between motor cortex and spinal motoneuronal pool during the performance of a maintained motor task in man. *J Physiol (Lond)* 489: 917-924, 1995.
doi: https://dx.doi.org/10.1113/jphysiol.1995.sp021104

Darling WG, Cole KJ, Abbs JH. Kinematic variability of grasp movements as a function of practice and movement speed. *Exp Brain Res* 73: 225-235, 1988.
doi: https://dx.doi.org/10.1007/BF00248215

Darling WG, Cole KJ. Muscle activation patterns and kinetics of human index finger movements. *J Neurophysiol* 63: 1098-1108, 1990.
doi: https://dx.doi.org/10.1152/jn.1990.63.5.1098

Denier van der Gon JJ, Thuring JP. The guiding of human writing movements. *Kybernetik* 2: 145-148, 1965.
doi: https://dx.doi.org/10.1007/BF00272310

Doeringer JA, Hogan N. Intermittency in preplanned elbow movements persists in the absence of visual feedback. *J Neurophysiol* 80: 1787-1799, 1998.
doi: https://dx.doi.org/10.1152/jn.1998.80.4.1787

Etz A, Gronau QF, Dablander F, Edelsbrunner PA, Baribault B. How to become a Bayesian in eight easy steps: An annotated reading list. *Psychon Bull Rev* 25: 219-234, 2018.
doi: https://dx.doi.org/10.3758/s13423-017-1317-5

Fishbach A, Roy SA, Bastianen C, Miller LE, Houk JC. Deciding when and how to correct a movement: Discrete submovements as a decision making process. *Exp Brain Res* 177: 45-63, 2007.
doi: https://dx.doi.org/10.1007/s00221-006-0652-y

Flash T. The organization of human arm trajectory control. In: *Multiple Muscle Systems: Biomechanics and Movement Organization*, edited by Winters JM, Woo SL-Y. New York, NY: Springer-Verlag, 1990, p. 282-301.
doi: https://dx.doi.org/10.1007/978-1-4613-9030-5_17

Flash T, Hogan N. The coordination of arm movements: An experimentally confirmed mathematical model. *J Neurosci* 5: 1688-1703, 1985.
doi: https://dx.doi.org/10.1523/JNEUROSCI.05-07-01688.1985

Freeman FN. Experimental analysis of the writing movement. *Psychol Rev Monogr* 17: 1-46, 1914.
doi: https://dx.doi.org/10.1037/h0093085

Freund H-J, Büdingen HJ. The relationship between speed and amplitude of the fastest voluntary contractions of human arm muscles. *Exp Brain Res* 31: 1-12, 1978.
doi: https://dx.doi.org/10.1007/BF00235800

Galganski ME, Fuglevand AJ, Enoka RM. Reduced control of motor output in a human hand muscle of elderly subjects during submaximal contractions. *J Neurophysiol* 69: 2108-2115, 1993.
doi: https://dx.doi.org/10.1152/jn.1993.69.6.2108

Gawthrop PJ, Loram ID, Lakie M, Gollee H. Intermittent control: A computational theory of human control. *Biol Cybern* 104: 31-51, 2011.
doi: https://dx.doi.org/10.1007/s00422-010-0416-4

Glencross DJ. The effects of changes in task conditions in the temporal organization of a repetitive speed skill. *Ergonomics* 18: 18-27, 1975.
doi: https://dx.doi.org/10.1080/00140137508931436

Gordon J, Ghez C. Trajectory control in targeted force impulses. II. Pulse height control. *Exp Brain Res* 67: 241-252, 1987.
doi: https://dx.doi.org/10.1007/BF00248546

Gross J, Timmermann L, Kujala J, Dirks M, Schmitz F, Salmelin R, Schnitzler A. The neural basis of intermittent motor control in humans. *Proc Natl Acad Sci USA* 99: 2299-2302, 2002.
doi: https://dx.doi.org/10.1073/pnas.032682099

Gruart A, Schreurs BG, del Toro ED, Delgado-García JM. Kinetic and frequency-domain properties of reflex and conditioned eyelid responses in the rabbit. *J Neurophysiol* 83: 836-852, 2000.
doi: https://dx.doi.org/10.1152/jn.2000.83.2.836

Guigon E. Active control of bias for the control of posture and movement. *J Neurophysiol* 104: 1090-1102, 2010.
doi: https://dx.doi.org/10.1152/jn.00162.2010

Guigon E, Baraduc P, Desmurget M. Computational motor control: Redundancy and invariance. *J Neurophysiol* 97: 331-347, 2007.
doi: https://dx.doi.org/10.1152/jn.00290.2006

Guigon E, Baraduc P, Desmurget M. Computational motor control: Feedback and accuracy. *Eur J Neurosci* 27: 1003-1016, 2008a
doi: https://dx.doi.org/10.1111/j.1460-9568.2008.06028.x

Guigon E, Baraduc P, Desmurget M. Optimality, stochasticity, and variability in motor behavior. *J Comput Neurosci* 24: 57-68, 2008b.
doi: https://dx.doi.org/10.1007/s10827-007-0041-y

Hallett M, Khoshbin S. A physiological mechanism of bradykinesia. *Brain* 103: 301-314, 1980.
doi: https://dx.doi.org/10.1093/brain/103.2.301

Harris CM, Wolpert DM. Signal-dependent noise determines motor planning. *Nature* 394: 780-784, 1998.
doi: https://dx.doi.org/10.1038/29528

Hernandez ME, Ashton-Miller JA, Alexander NB. The effect of age, movement direction, and target size on the maximum speed of targeted COP movements in healthy women. *Hum Mov Sci* 31: 1213-1223, 2012.
doi: https://dx.doi.org/10.1016/j.humov.2011.11.002

Hoff B, Arbib MA. Models of trajectory formation and temporal interaction of reach and grasp. *J Mot Behav* 25: 175-192, 1993.
doi: https://dx.doi.org/10.1080/00222895.1993.9942048

Jaberzadeh S, Brodin P, Flavel SC, O'Dwyer NJ, Nordstrom MA, Miles TS. Pulsatile control of the human masticatory muscles. *J Physiol (Lond)* 547: 613-620, 2003.
doi: https://dx.doi.org/10.1113/jphysiol.2003.030221

JASP Team. JASP 2018 (Version 0.8.5)[Computer software].
link: https://jasp-stats.org/

Jeannerod M. The timing of natural prehension movements. *J Mot Behav* 16: 235-254, 1984.
doi: https://dx.doi.org/10.1080/00222895.1984.10735319

Karniel A. The minimum transition hypothesis for intermittent hierarchical motor control. *Front Comput Neurosci* 7: 12, 2013.
doi: https://dx.doi.org/10.3389/fncom.2013.00012

Kelso JAS. *Dynamic Patterns*. Cambridge, MA: MIT Press, 1995.
isbn: http://www.isbnsearch.org/isbn/9780262611312

Krebs HI. Robot-aided neuro-rehabilitation and functional imaging. PhD Thesis, Massachusetts Institute of Technology, Cambridge, MA, 1997.
Available from: http://hdl.handle.net/1721.1/10308

Krebs HI, Aisen ML, Volpe BT, Hogan N. Quantization of continuous arm movements in humans with brain injury. *Proc Natl Acad Sci USA* 96: 4645-4649, 1999.
doi: https://dx.doi.org/10.1073/pnas.96.8.4645

Lee D, Port NL, Georgopoulos AP. Manual interception of moving targets. II. On-line control of overlapping submovements. *Exp Brain Res* 116: 421-433, 1997.
doi: https://dx.doi.org/10.1007/PL00005770

Levy-Tzedek S, Krebs H, Song D, Hogan N, Poizner H. Non-monotonicity on a spatio-temporally defined cyclic task: Evidence of two movement types? *Exp Brain Res* 202: 733-746, 2010.
doi: https://dx.doi.org/10.1007/s00221-010-2176-8

Li Z, Mazzoni P, Song S, Qian N. A single, continuously applied control policy for modeling reaching movements with and without perturbation. *Neural Comput* 30: 397-427, 2018.
doi: https://dx.doi.org/10.1162/neco_a_01040

Liu D, Todorov E. Evidence for the flexible sensorimotor strategies predicted by optimal feedback control. *J Neurosci* 27: 9354-9368, 2007.
doi: https://dx.doi.org/10.1523/JNEUROSCI.1110-06.2007

Loram ID, Lakie M. Human balancing of an inverted pendulum: Position control by small, ballistic-like, throw and catch movements. *J Physiol (Lond)* 540: 1111-1124, 2002.
doi: https://dx.doi.org/10.1113/jphysiol.2001.013077

McAuley JH, Farmer SF, Rothwell JC, Marsden CD. Common 3 and 10 Hz oscillations modulate human eye and finger movements while they simultaneously track a visual target. *J Physiol (Lond)* 515: 905-917, 1999a.
doi: https://dx.doi.org/10.1111/j.1469-7793.1999.905ab.x

McAuley JH, Rothwell JC, Marsden CD. Human anticipatory eye movements may reflect rhythmic central nervous activity. *Neuroscience* 94: 339-350, 1999b.
doi: https://dx.doi.org/10.1016/S0306-4522(99)00337-1

Messier J, Adamovich S, Berkinblit M, Tunik E, Poizner H. Influence of movement speed on accuracy and coordination of reaching movements to memorized targets in three-dimensional space in a deafferented subject. *Exp Brain Res* 150: 399-416, 2003.
doi: https://dx.doi.org/10.1007/s00221-003-1413-9

Meyer DE, Abrams RA, Kornblum S, Wright CE, Smith JEK. Optimality in human motor performance: Ideal control of rapid aimed movement. *Psychol Rev* 95: 340-370, 1988.
doi: https://dx.doi.org/10.1037/0033-295x.95.3.340

Miall RC, Weir DJ, Stein JF. Visuomotor tracking with delayed visual feedback. *Neuroscience* 16: 511-520, 1985.
doi: https://dx.doi.org/10.1016/0306-4522(85)90189-7

Miall RC, Weir DJ, Stein JF. Manual tracking of visual targets by trained monkeys. *Behav Brain Res* 20: 185-201, 1986.
doi: https://dx.doi.org/10.1016/0166-4328(86)90003-3

Michmizos KP, Krebs HI. Pointing with the ankle: The speed-accuracy trade-off. *Exp Brain Res* 232: 647-657, 2014.
doi: https://dx.doi.org/10.1007/s00221-013-3773-0

Milner TE, Ijaz MM. The effect of accuracy constraints on three-dimensional movement kinematics. *Neuroscience* 35: 365-374, 1990.
doi: https://dx.doi.org/10.1016/0306-4522(90)90090-Q

Morasso P, Mussa-Ivaldi F, Ruggiero C. How a discontinuous mechanism can produce continuous patterns in trajectory formation and handwriting. *Acta Psychol (Amst)* 54: 83-98, 1983.
doi: https://dx.doi.org/10.1016/0001-6918(83)90025-2

Navas F, Stark L. Sampling or intermittency in hand control system dynamics. *Biophys J* 8: 252-302, 1968.
doi: https://dx.doi.org/10.1016/S0006-3495(68)86488-4

Neilson PD, Neilson MD, O'Dwyer NJ. Internal models and intermittency: A theoretical account of human tracking behavior. *Biol Cybern* 58: 101-112, 1988.
doi: https://dx.doi.org/10.1007/BF00364156

Nelson WL. Physical principles for economies of skilled movements. *Biol Cybern* 46: 135-147, 1983.
doi: https://dx.doi.org/10.1007/BF00339982

Oldfield RC. The assessment and analysis of handeness: The Edinburgh inventory. *Neuropsychologia* 9: 97-113, 1971.
doi: https://dx.doi.org/10.1016/0028-3932(71)90067-4

Park SW, Marino H, Charles SK, Sternad D, Hogan N. Moving slowly is hard for humans: Limitations of dynamic primitives. *J Neurophysiol* 118: 69-83, 2017.
doi: https://dx.doi.org/10.1152/jn.00643.2016

Qian N, Jiang Y, Jiang ZP, Mazzoni P. Movement duration, Fitts's law, and an infinite-horizon optimal feedback control model for biological motor systems. *Neural Comput* 25: 697-724, 2013.
doi: https://dx.doi.org/10.1162/NECO_a_00410

Rand MK, Shimansky YP. Two-phase strategy of neural control for planar reaching movements: II. Relation to spatiotemporal characteristics of movement trajectory. *Exp Brain Res* 230: 1-13, 2013.
doi: https://dx.doi.org/10.1007/s00221-013-3626-x

Rigoux L, Guigon E. A model of reward- and effort-based optimal decision making and motor control. *PLoS Comput Biol* 8: e1002716, 2012.
doi: https://dx.doi.org/10.1371/journal.pcbi.1002716

Sakaguchi Y, Tanaka M, Inoue Y. Adaptive intermittent control: A computational model explaining motor intermittency observed in human behavior. *Neural Netw* 67: 92-109, 2015.
doi: https://dx.doi.org/10.1016/j.neunet.2015.03.012

Salmond LH. Characterization of smoothness in wrist rotations. M. Sc. Thesis, Brigham Young University, 2014.
Available from: http://hdl.lib.byu.edu/1877/etd7413

Salmond LH, Davidson AD, Charles SK. Proximal-distal differences in movement smoothness reflect differences in biomechanics. *J Neurophysiol* 117: 1239-1257, 2017.
doi: https://dx.doi.org/10.1152/jn.00712.2015

Sartori L, Camperio-Ciani A, Bulgheroni M, Castiello U. Reach-to-grasp movements in Macaca fascicularis monkeys: The isochrony principle at work. *Front Psychology* 4: 114, 2013.
doi: https://dx.doi.org/10.3389/fpsyg.2013.00114

Shaikh AG, Wong A, Zee DS, Jinnah HA. Why are voluntary head movements in cervical dystonia slow? *Parkinsonism Relat Disord* 21: 561-566, 2015.
doi: https://dx.doi.org/10.1016/j.parkreldis.2015.03.005

Shaffer LH. Rhythm and timing in skill. *Psychol Rev* 89: 109-122, 1982.
doi: https://dx.doi.org/10.1037/0033-295X.89.2.109

Shmuelof L, Krakauer JW, Mazzoni P. How is a motor skill learned? Change and invariance at the levels of task success and trajectory control. *J Neurophysiol* 108: 578-594, 2012.
doi: https://dx.doi.org/10.1152/jn.00856.2011

Stetson RH, McDill JA. Mechanism of the different types of movement. *Psychol Monogr* 32: 18-40, 1923.
doi: https://dx.doi.org/10.1037/h0093206

Terzuolo C, Viviani P. Determinants and characteristics of motor patterns used for typing. *Neuroscience* 5: 1085-1103, 1980.
doi: https://dx.doi.org/10.1016/0306-4522(80)90188-8

Todorov E. Optimality principles in sensorimotor control. *Nat Neurosci* 7: 907-915, 2004. doi: https://dx.doi.org/10.1038/nn1309

Todorov E. Stochastic optimal control and estimation methods adapted to the noise characteristics of the sensorimotor system. *Neural Comput* 17: 1084-1108, 2005. doi: https://dx.doi.org/10.1162/0899766053491887

Todorov E, Jordan MI. Optimal feedback control as a theory of motor coordination. *Nat Neurosci* 5: 1226-1235, 2002. doi: https://dx.doi.org/10.1038/nn963

Torres EB, Andersen R. Space-time separation during obstacle-avoidance learning in monkeys. *J Neurophysiol* 96: 2613-2632, 2006. doi: https://dx.doi.org/10.1152/jn.00188.2006

Torres EB, Zipser D. Simultaneous control of hand displacements and rotations in orientation-matching experiments. *J Appl Physiol* 96: 1978-1987, 2004. doi: https://dx.doi.org/10.1152/japplphysiol.00872.2003

Uno Y, Kawato M, Suzuki R. Formation and control of optimal trajectory in human multijoint arm movement - minimum torque change model. *Biol Cybern* 61: 89-101, 1989. doi: https://dx.doi.org/10.1007/BF00204593

Vallbo AB, Wessberg J. Organization of motor output in slow finger movements. *J Physiol (Lond)* 469: 673-691, 1993. doi: https://dx.doi.org/10.1113/jphysiol.1993.sp019837

van der Wel RPRD, Sternad D, Rosenbaum DA. Moving the arm at different rates: Slow movements are avoided. *J Mot Behav* 42: 29-36, 2009. doi: https://dx.doi.org/10.1080/00222890903267116

Viviani P, Terzuolo C. Trajectory determines movement dynamics. *Neuroscience* 7: 431-437, 1982. doi: https://dx.doi.org/10.1016/0306-4522(82)90277-9

Wadman WJ, Denier van der Gon JJ, Geuze RH, Mol CR. Control of fast goal-directed arm movements. *J Hum Mov Stud* 5: 3-17, 1979.

Warabi T, Noda H, Yanagisawa N, Tashiro K, Shindo R. Changes in sensorimotor functions associated with the degree of bradykinesia of Parkinson's disease. *Brain* 109: 1209-1224, 1986. doi: https://dx.doi.org/10.1093/brain/109.6.1209

Welsh JP, Llinás R. Some organizing principles for the control of movement based on olivocerebellar physiology. *Prog Brain Res* 114: 449-461, 1997. doi: https://dx.doi.org/10.1016/S0079-6123(08)63380-4

Williams ER, Soteropoulos DS, Baker SN. Coherence between motor cortical activity and peripheral discontinuities during slow finger movements. *J Neurophysiol* 102: 1296-1309, 2009.
doi: https://dx.doi.org/10.1152/jn.90996.2008

Williams ER, Soteropoulos DS, Baker SN. Spinal interneuron circuits reduce approximately 10-Hz movement discontinuities by phase cancellation. *Proc Natl Acad Sci USA* 107: 11098-11103, 2010.
doi: https://dx.doi.org/10.1073/pnas.0913373107

Figure captions

Figure 1. **A**. Schematic properties of segmented movements. (*left*) Velocity profiles of movements of 4 different durations (*black*, short — *red*/*green*, intermediate — *blue*, long). (*right*) Number of velocity peaks as function of movement duration. **B**. Schematic properties of smooth movements. Velocity profiles were built with the minimum-jerk model. A minimum-jerk trajectory is defined by a duration *D* and initial and final (boundary) conditions ($\mathrm{pos_i}$, $\mathrm{vel_i}$, $\mathrm{acc_i}$, $\mathrm{pos_f}$, $\mathrm{vel_f}$, $\mathrm{acc_f}$). Units are arbitrary. **A** (*black*) *D* = 0.5 and (0, 0, 0, 1, 0, 0). **A** (*red*) *D* = 0.5 and (0, 0, 0, 0.5, 0.5, 0) + *D* = 0.5 and (0.5, 0.5, 0, 1, 0, 0). **A** (*green*) *D* = 0.55 and (0, 0, 0, 0.33, 0.25, 0) + *D* = 0.55 and boundary conditions (0.33, 0.25, 0, 0.66, 0.25, 0) + *D* = 0.55 and boundary conditions (0.66, 0.25, 0, 1, 0, 0). **A** (*blue*) *D* = 0.6 and boundary conditions (0, 0, 0, 0.25, 0.25, 0) + *D* = 0.6 and boundary conditions (0.25, 0.25, 0, 0.5, 0.25, 0) + *D* = 0.6 and boundary conditions (0.5, 0.25, 0, 0.75, 0.25, 0) + *D* = 0.6 and boundary conditions (0.75, 0.25, 0, 1, 0, 0). **B** (*black*) *D* = 0.6 and boundary conditions (0, 0, 0, 1, 0, 0). **B** (*red*) *D* = 1.2 and boundary conditions (0, 0, 0, 1, 0, 0). **B** (*green*) *D* = 1.8 and boundary conditions (0, 0, 0, 1, 0, 0). **B** (*blue*) *D* = 2.4 and boundary conditions (0, 0, 0, 1, 0, 0). The properties of segmented movements correspond to what was known before the present study (velocity fluctuations, scaling of the number of velocity peaks with movement duration).

Figure 2. **A**. Experimental setup. **B**. Example of velocity profile (participant NH, movement speed 4.71 cm/s). The *white box* (*gray box*) indicates a left-to-right (right-to-left) movement. Vertical dashed lines are the limits of segments (minima of velocity). **C**. Schematic representation of a segment of velocity with 4 units, i.e. 4 peaks of acceleration (see **D**). **D**. Acceleration (derivative of the velocity segment in **C**). There are 4 peaks in the acceleration profile. **E**. Jerk (derivative of the acceleration segment in **D**). **F**. Another

segment of velocity with 4 units. In this case there are only 3 peaks of acceleration (see **G**). **G**. Acceleration (derivative of **F**). There are 3 peaks in the acceleration profile, but the acceleration profile is highly irregular (*arrow*). **H**. Jerk (derivative of **G**). A peak of jerk is observed before the beginning of the segment and is responsible for the irregular initial acceleration (see **G**).

Figure 3. Data for participant NH, movement speed 2.35 cm/s. **A**. Distribution of N_{unit}. **B**. Relationship between mean segment duration (*dot*) and N_{unit}. The central mark in the box is the median, the edges of the box are the 25th and 75th percentiles, the whiskers extend to the most extreme data points not considered outliers. **C**. Distribution of segment duration. **D**. Relationship between mean segment velocity and N_{unit}. Same conventions as in **B**.

Figure 4. Data for participant NH. **A**. Distribution of N_{unit} for the 8 task conditions. **B**. Relationship between mean segment duration and movement speed for 2-unit (*black*), 3-unit (*red*), 4-unit (*green*) and 5-unit (*blue*) segments. Bar indicates standard deviation. **C**. Relationship between mean segment velocity and movement speed. Standard deviation divided by 7 for legibility. Colored lines correspond to linear regression ($R^2 = 0.98, 0.92, 0.62, 0.64$).

Figure 5. **A**. Power spectral density function (smoothed with 5-point moving average) of the acceleration signal (participant TV). Color code for movement speed (see **B**). Vertical dashed lines indicate peak frequency. **B**. Peak frequency of the power spectral density function for all participants (open symbols) and all conditions (colors). Horizontal dashed line indicates mean frequency.

Figure 6. Simulation of the noise-free model. **A**. Position (*black*, 1 cm/s — *dark gray*, 2 cm/s — *gray*, 5 cm/s — *light gray*, 10 cm/s). The staircase trace is the goal position for the movement at 10 cm/s. **B**. Velocity profile. The constant trace is the goal velocity for the movement at 10 cm/s. **C**. Duration of segments. **D**. Velocity of segments.

Figure 7. Simulation of the model with noise and comparison with an average participant. **A**. Distribution of N_{unit} for the 4 simulated conditions (*gray bars*; see Fig. 6) and 8 task conditions (*colored lines*; see Fig. 5). **B**. Relationship between mean segment duration and movement speed for 2-unit (*square*), 3-unit (*diamond*), 4-unit (*up triangle*) and 5-unit (*down triangle*) segments. Bar indicates standard deviation. Grays and colors as in **A**. **C**. Relationship between mean segment velocity and movement speed for 2-unit segments. **D**. Same as **C** for 3-unit segments. **E**. Same as **C** for 4-unit segments. **F**. Same as **C** for 5-unit segments.

Figure 8. Simulation of the model with noise and comparison with an average participant. **A**. Slope, intercept and R^2 of the linear regression between N_{unit} and segment duration. **B**. Slope, intercept and R^2 of the linear regression between N_{unit} and segment velocity. Same color code as in Fig. 7.

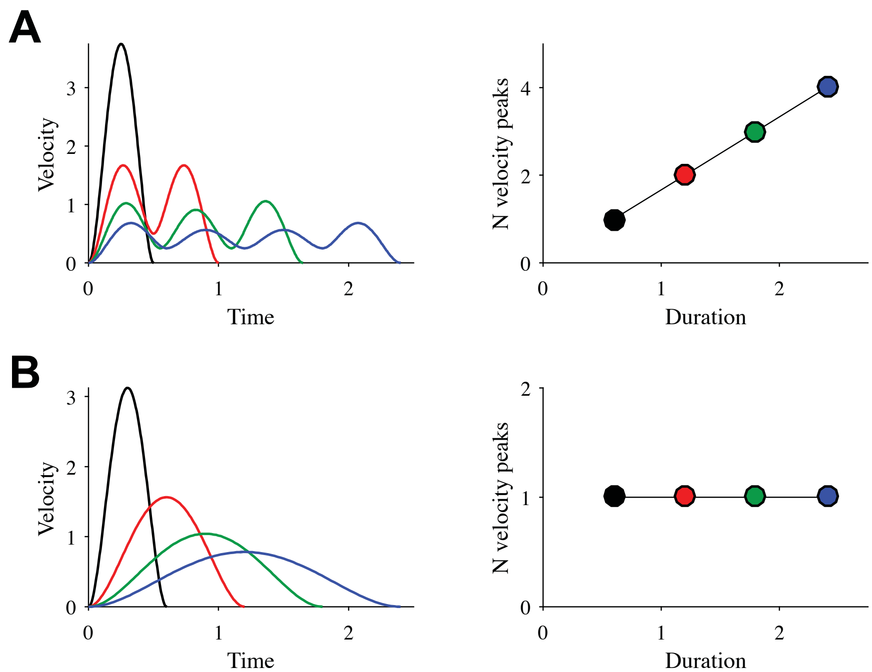

Figure 1

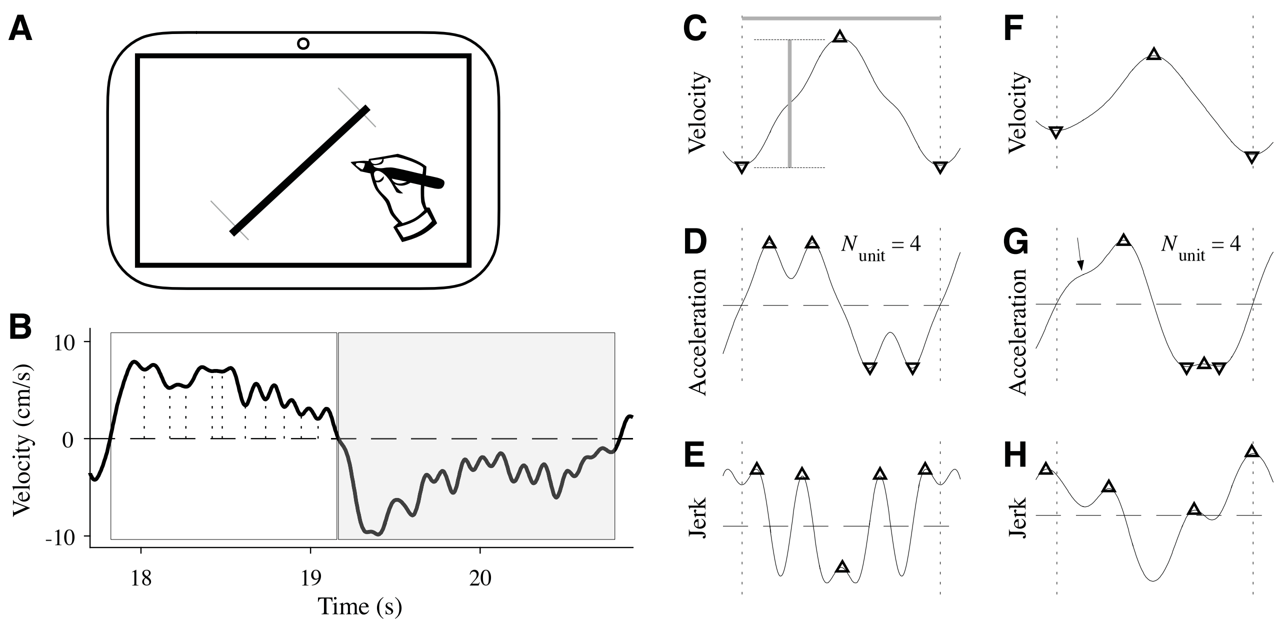
A
B
Velocity (cm/s)
10
0
-10
18
19
20
Time (s)
C
Velocity
D
Acceleration
$N_{unit} = 4$
E
Jerk
F
Velocity
G
Acceleration
$N_{unit} = 4$
H
Jerk

Figure 2

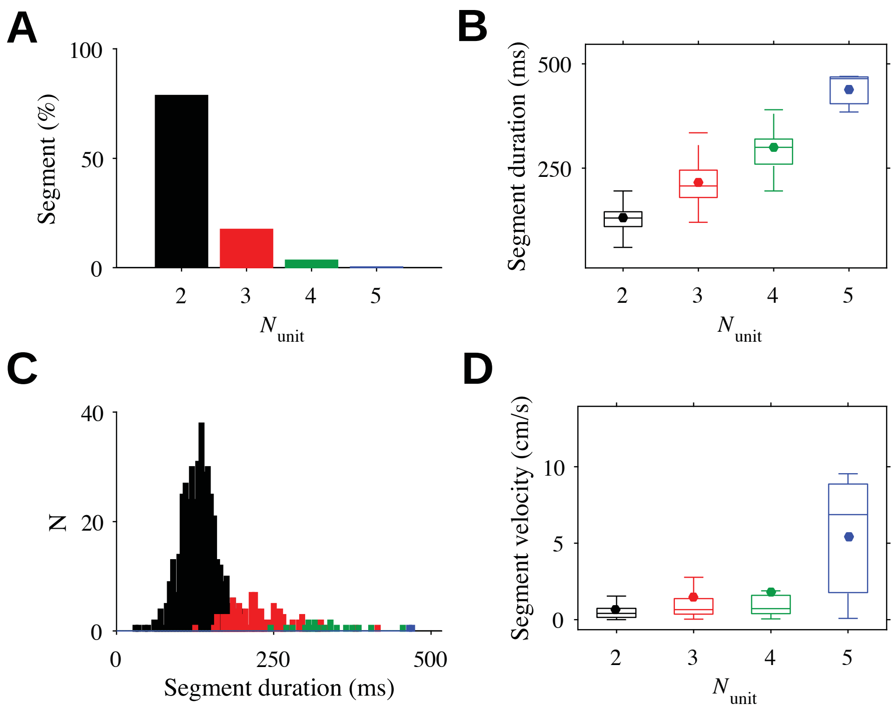

A
100
50
0
Segment (%)
2
3
4
5
N unit
B
500
250
Segment duration (ms)
2
3
4
5
N unit
C
40
20
0
N
0
250
500
Segment duration (ms)
D
10
5
0
Segment velocity (cm/s)
2
3
4
5
N unit

Figure 3

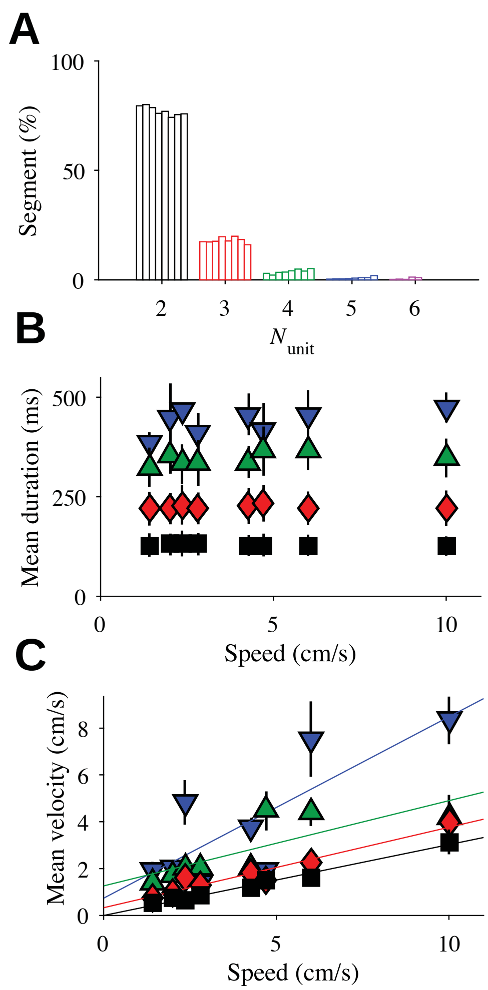
A
100
Segment (%)
50
0
2
3
4
5
6
N_{unit}
B
500
Mean duration (ms)
250
0
0
5
10
Speed (cm/s)
C
8
6
Mean velocity (cm/s)
4
2
0
0
5
10
Speed (cm/s)

Figure 4

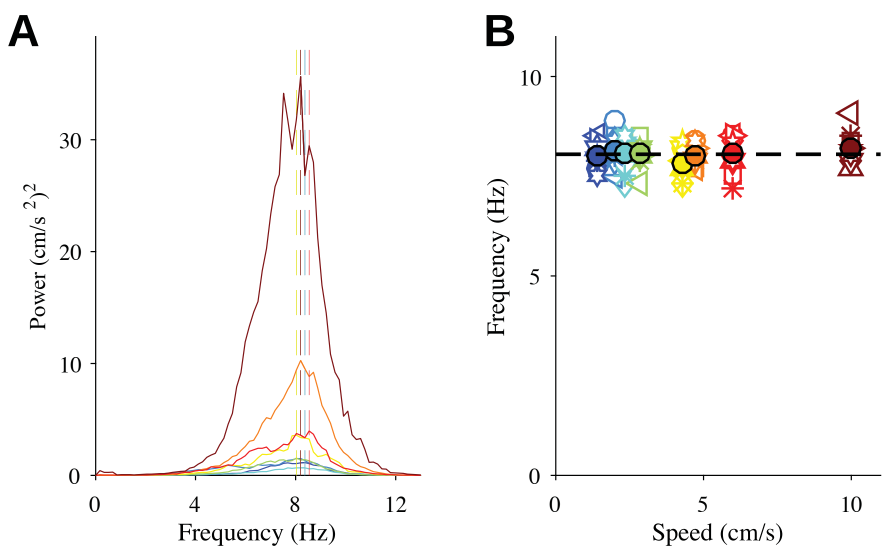
A
Power (cm/s ^{2})^2
30
20
10
0
0
4
8
12
Frequency (Hz)
B
10
5
0
Frequency (Hz)
0
5
10
Speed (cm/s)

Figure 5

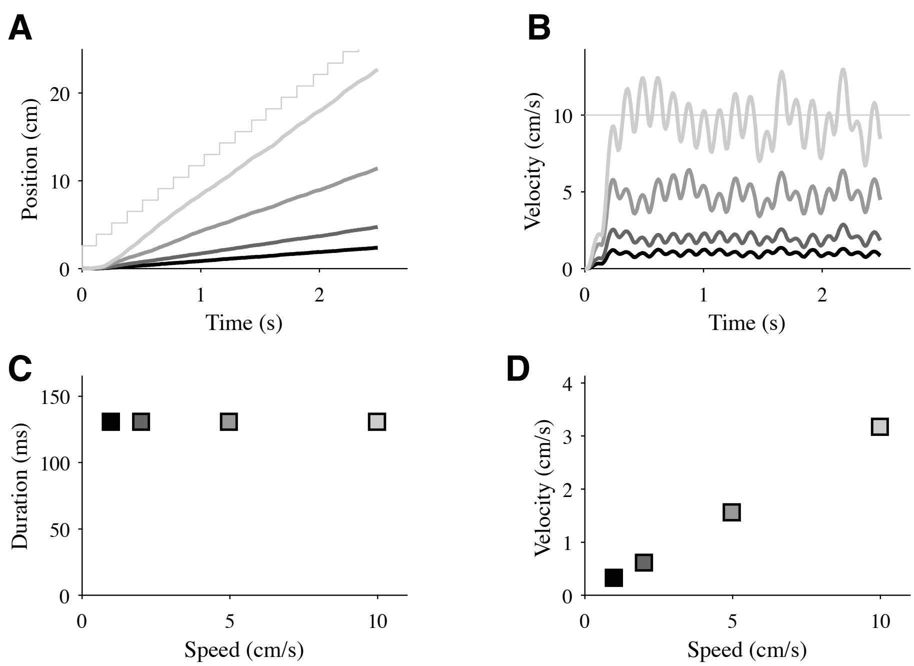
A
B
C
D
Position (cm)
Time (s)
Velocity (cm/s)
Time (s)
Duration (ms)
Speed (cm/s)
Velocity (cm/s)
Speed (cm/s)

Figure 6

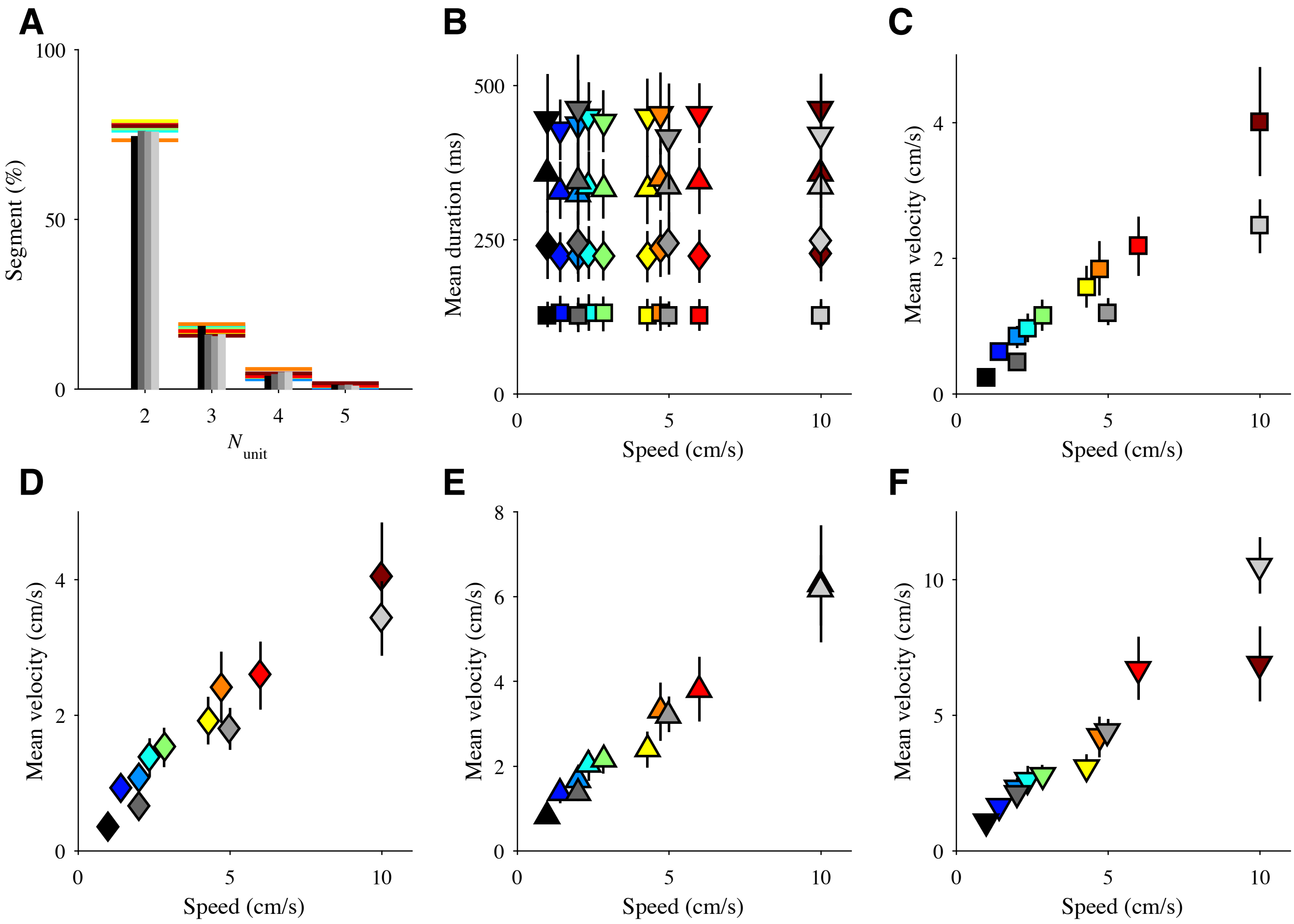
A
100
50
0
Segment (%)
2
3
4
5
N unit
B
500
250
0
Mean duration (ms)
0
5
10
Speed (cm/s)
C
4
2
0
Mean velocity (cm/s)
0
5
10
Speed (cm/s)
D
4
2
0
Mean velocity (cm/s)
0
5
10
Speed (cm/s)
E
8
6
4
2
0
Mean velocity (cm/s)
0
5
10
Speed (cm/s)
F
10
5
0
Mean velocity (cm/s)
0
5
10
Speed (cm/s)

Figure 7

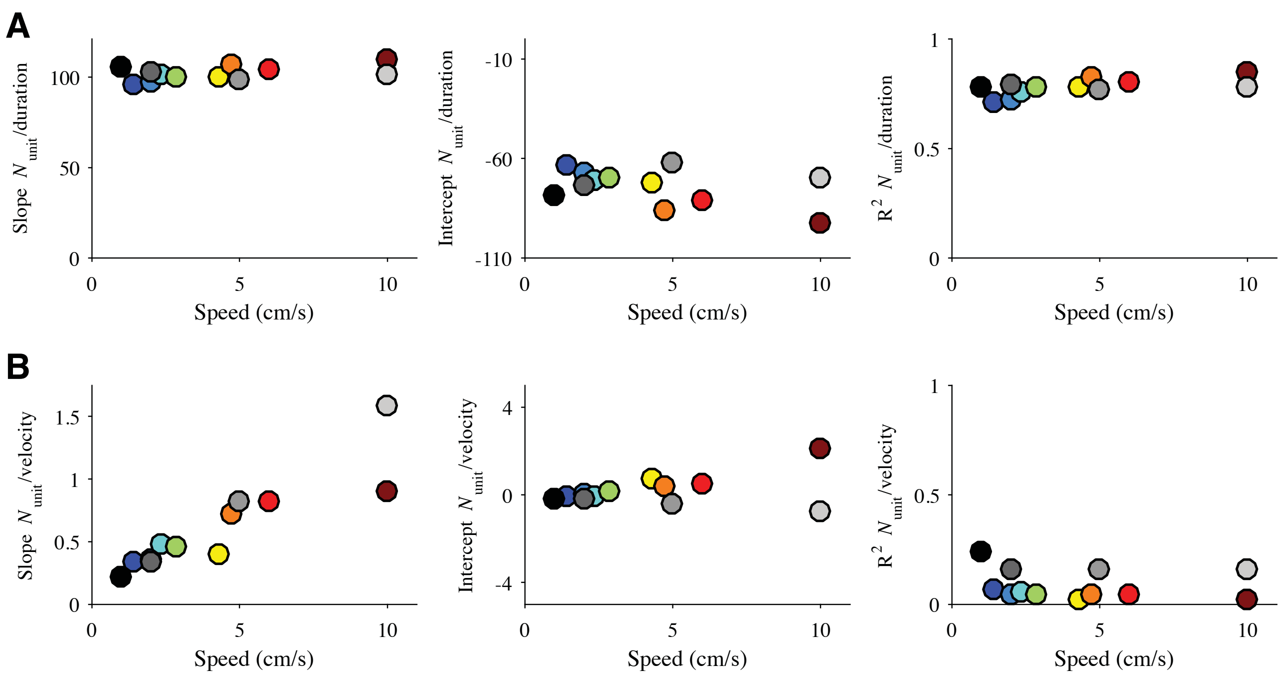
A
Slope N_{unit}/duration
Speed (cm/s)
Intercept N_{unit}/duration
Speed (cm/s)
R^2 N_{unit}/duration
Speed (cm/s)
B
Slope N_{unit}/velocity
Speed (cm/s)
Intercept N_{unit}/velocity
Speed (cm/s)
R^2 N_{unit}/velocity
Speed (cm/s)

Figure 8